JOURNAL OF MATERIALS SCIENCE 26 (1991) 909–916

Pulsed laser processing of thermal barrier coatings

K. MOHAMMED JASIM*, R. D. RAWLINGS, D. R. F. WEST
Department of Materials, Imperial College of Science, Medicine and Technology, Exhibition Road, London SW7 2BP, UK

Results are reported of the effects of surface melting (sealing) produced by a 1 kW laser in pulsed mode on the structure of plasma-sprayed 8 wt% yttria partially stabilized zirconia (YPSZ); pulse lengths in the range of 1 to 90 msec were used. Smooth surfaces were produced with shallow cracks at values of laser energy 5 to 40 J. Comparison of the data is made with results obtained by sealing using continuous wave CO_2 laser processing.

1. Introduction

Ceramics are extensively used for coating components in order to enhance the performance by improving properties such as corrosion, erosion and electrical resistance. Ceramic thermal barrier coatings are used to provide insulation to critical metal components in turbine, utility and diesel engines [1]. The most widely employed ceramics for thermal barrier coatings are zirconias containing varying amounts of the stabilizing oxides CaO, MgO and Y_2O_3 [2, 3]. The most commonly encountered are the zirconias containing of the order of 6 to 12 wt % yttria; these are known as yttria partially stabilized zirconias (YPSZs) and have unique thermal properties, namely a low thermal conductivity, which is effectively invariant with temperature, and a high thermal expansion coefficient [4]. Typically, yttria-stabilized zirconia powders are applied to metal substrates by thermal spraying processes such as plasma spraying and the resulting coatings contain a high volume fraction of porosity, voids and cracks [5, 6]. Although the presence of porosity may be beneficial as far as thermal insulation is concerned [7], this is out-weighed by the associated disadvantages. The porosity and cracks permit contaminants in the fuel to penetrate the coating which can lead to destabilization of the coating and attack on the intermediate layer between the component and the thermal barrier coat, known as the bond coat [8, 9]. Also the poor surface finish of the plasma-sprayed coating is not aerodynamically smooth. A few investigations have been carried out of the feasibility of using high-power energy beams to optimize the properties of plasma-sprayed layers by decreasing the porosity and improving the surface finish [10–17]. High-power beams such as ion beams and lasers have been studied, but lasers have many advantages compared with ion beams, in particular being more economic and not requiring a vacuum.

There are two modes of operations of lasers; these are known as continuous wave (CW) and pulsed modes (P_s). As the name suggests, in the CW mode the laser is in continuous operation and the time that the beam is in contact with a given area of the work piece (i.e. interaction time) is given by the diameter of the beam divided by the relative scan speed of the work piece and the laser beam. In the single pulsed mode the peak power, which is a function of both pulse width and frequency can be considerably higher than in the CW mode. The combination of high power density and short interaction time results in high temperature gradients. Consequently the rate of cooling during solidification is very rapid in the pulsed mode. Furthermore, the extent of evaporation is negligible for short pulse duration. Previous investigations [10–16] of laser melting of plasma-sprayed zirconias have mainly used a continuous wave CO_2 laser; for example, our previous work [10, 11, 15, 16] on plasma-sprayed, ZrO_2–30 wt % CaO, ZrO_2–8 wt % Y_2O_3, ZrO_2–20 wt % Y_2O_3 and ZrO_2–6.5 wt % Y_2O_3–10 wt % Al_2O_3. These and other studies [12, 14] have been concerned with the effect of laser processing parameters on the microstructure, surface finish and crack density and morphology. It has been demonstrated that laser sealing with an acceptable surface finish can be achieved using the CW mode, although the sealed surface has a network of cracks with some additional small secondary cracks. Laser sealing has been reported to give a four-fold improvement in cyclic corrosion tests in a burner rig [13] but this was not confirmed in oxidation tests.

Fewer investigations of sealing have been made using the pulsed mode. Dallaire and Cielo [18] have reported the results of a study of the effect of a CO_2 pulsed laser used at different power densities on a nickel plasma-sprayed coating on a steel substrate. It was concluded that the minimum pulse duration for sealing the layer was a pulse in the range of 20 to 40 μsec. A semi-infinite one-dimensional heat flow model was used to calculate the temperature and depth of sealing. Sivakumar and Mordike [14] studied

*Permanent address: Scientific Research Council, Baghdad, Iraq.

0022–2461/90 $03.00 + .12 © 1990 Chapman and Hall Ltd.

the effect of laser process parameters on the surface melting of various ceramic coatings based on ZrO_2, Al_2O_3 and TiO_2, using both CW and pulsed modes. The ZrO_2-based ceramics were stabilized with 5 wt % CaO, 21 wt % MgO and 6 and 20 wt % Y_2O_3. The pulsed mode was used with a peak power density of 10^3 to 10^4 W mm^{-2} with pulse lengths varying from 0.03 to 0.4 msec and a beam diameter of 0.4 mm. Pulsed mode parameters (i.e. frequency, pulse duration and pulse separation) could be adjusted to give a range of depths of sealing and crack morphology; shallow depth of melting showed only transverse cracks, which can be beneficial in the accommodation of stresses, in contrast increased depth of sealing gave cracks which led to spalling. Generally the ZrO_2-based coatings were found to be more prone to cracking than the other coatings.

The present paper summarizes the results of an investigation using a pulsed CO_2 laser to seal a YPSZ plasma-sprayed layer. The results are compared with results of laser sealing produced by a CW CO_2 laser.

2. Experimental procedure

The substrate was a mild steel in the form of 25.4 mm diameter, 6 mm thick discs. The upper surface of the discs was shot blasted with alumina to increase the adherence between the bond layer and the substrate. The samples were first sprayed with a nickel-based bond layer and then with 8 wt % YPSZ powder, using argon and hydrogen as primary and secondary gases, respectively. The thickness of the bond layer was ~ 80 μm and the thickness of the ceramic layer was ~ 250 μm. A 1 kW pulsed CO_2 laser (Ferranti MFK1) was used to seal the layer. The sprayed samples were fixed perpendicular to a 3.9 mm diameter laser beam; single pulses were used at different pulse length and hence different specific energy, where the specific energy = power density × pulse length (Table I).

TABLE I Laser parameters studied

Power, P	1 kW
Laser beam diameter, D	3.9 mm
Pulse length	1–90 msec
Power density, P_d	83.7 W mm^{-2}
Specific energy, S	0.082–7.55 J mm^{-2}
Energy, E	1–90 J
Beam mode	doughnut
No argon shroud was used	

After laser sealing, the dimensions (width and depth) of the sealed region were measured and the microstructural features such as dimensions of surface depressions, crack density, crack width, spacing of cracks and cell size were recorded. All studies, includ-

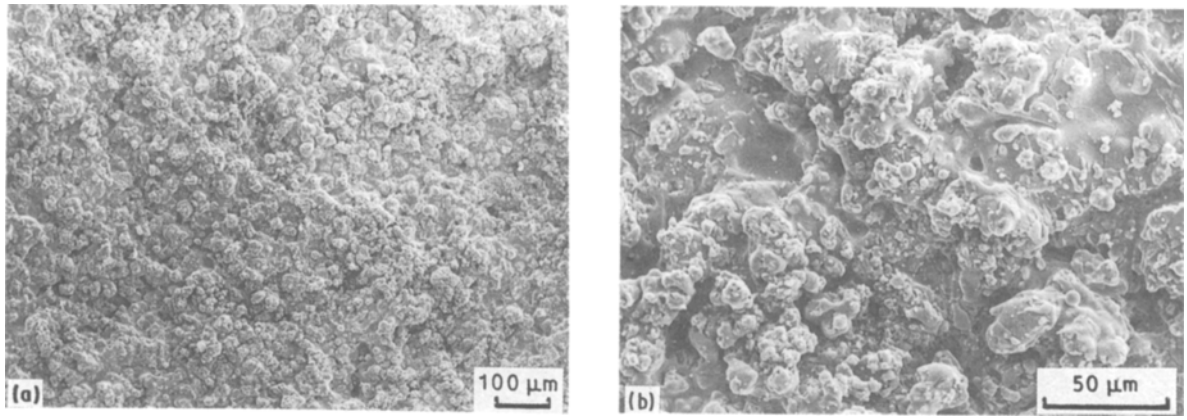

Figure 1 Scanning electron micrographs of plan view of as-sprayed 8 wt % YSZ: (a) showing the general appearance, and (b) higher magnification showing the presence of cracks and porosity.

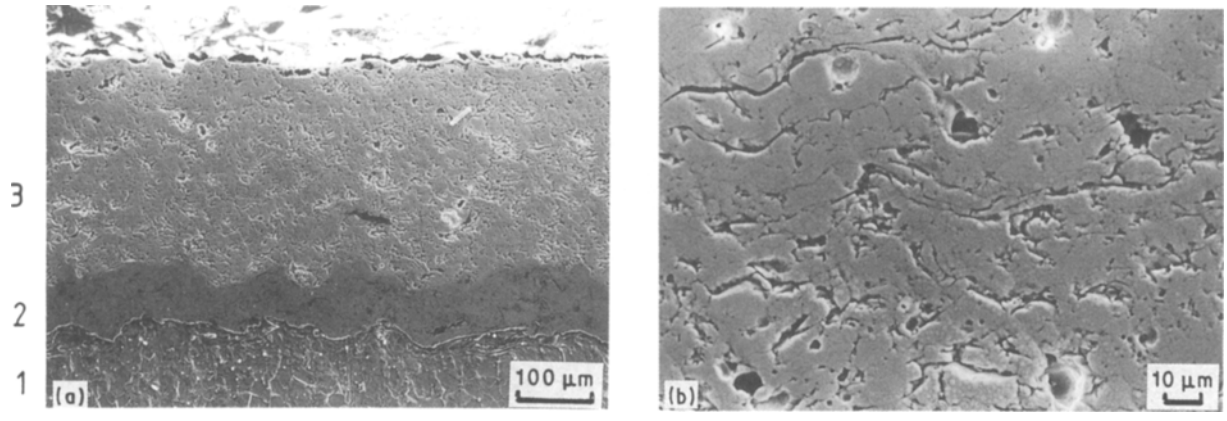

Figure 2 Scanning electron micrographs of transverse section of as-sprayed thermal coating system. (a) Low magnification showing: 1, substrate; 2, bond layer; and 3, ceramic layer. (b) Higher magnification of the ceramic layer showing the presence of closed porosity.

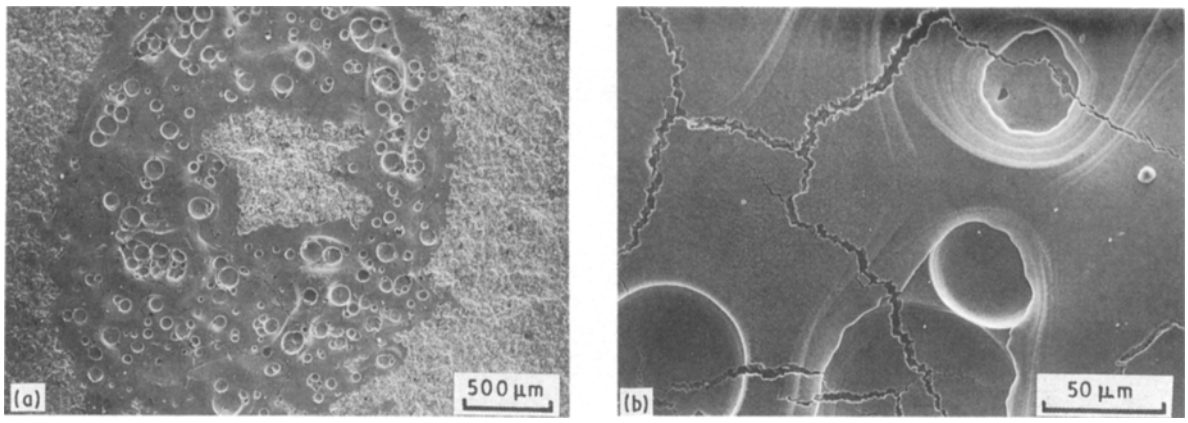

Figure 3 General appearance of plan view of single pulse, energy 5 J: (a) low magnification and (b) higher magnification showing the presence of depressions.

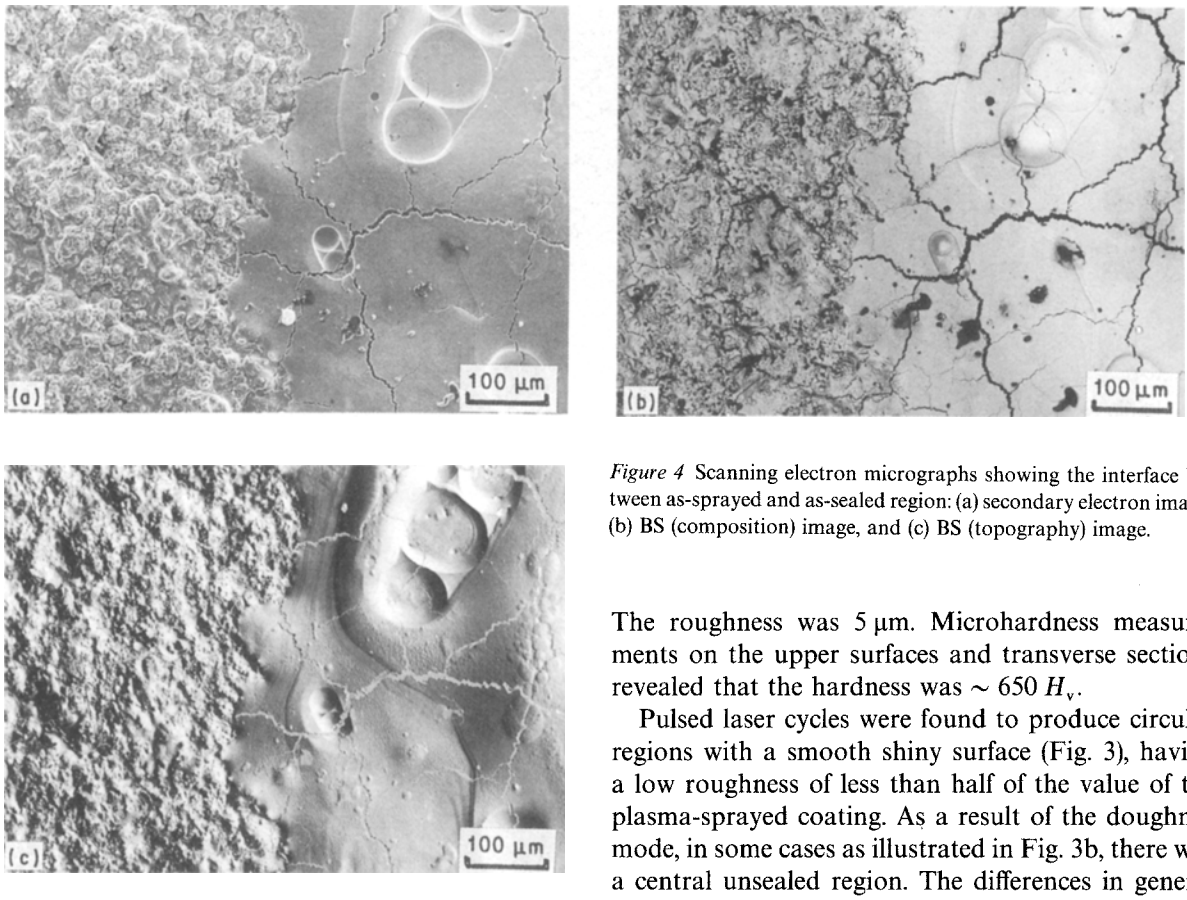

Figure 4 Scanning electron micrographs showing the interface between as-sprayed and as-sealed region: (a) secondary electron image, (b) BS (composition) image, and (c) BS (topography) image.

ing the dimensional measurements, were made using a scanning electron microscope. Roughness measurements were made with a Talysurf and quantified in terms of centre-line average values. Hardness measurements were carried out at 300 and 500 g load for as-sealed and as-sprayed layers respectively.

3. Results and discussion

In order to study the effect of laser pulsing on the plasma-sprayed ceramic, the as-sprayed layer was first evaluated for porosity, voids, roughness, cracks and hardness. Figs 1 and 2 show the general appearance of plan views and transverse sections of plasma-sprayed material; a high volume fraction of porosity together with many primary and secondary cracks are evident. The roughness was 5 μm. Microhardness measurements on the upper surfaces and transverse sections revealed that the hardness was $\sim 650\ H_v$.

Pulsed laser cycles were found to produce circular regions with a smooth shiny surface (Fig. 3), having a low roughness of less than half of the value of the plasma-sprayed coating. As a result of the doughnut mode, in some cases as illustrated in Fig. 3b, there was a central unsealed region. The differences in general

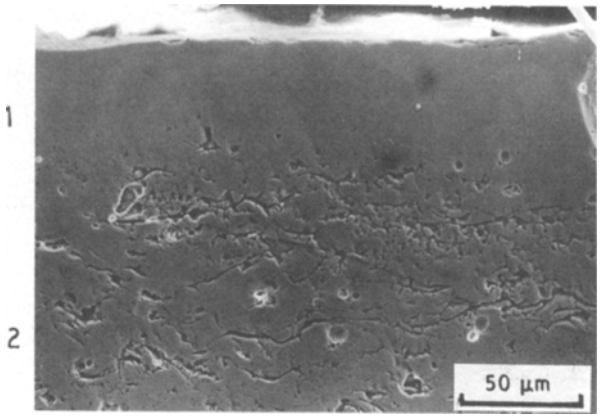

Figure 5 Transverse section of as-sealed layer processed at 10 J. 1, sealed zone; 2, original ceramic layer.

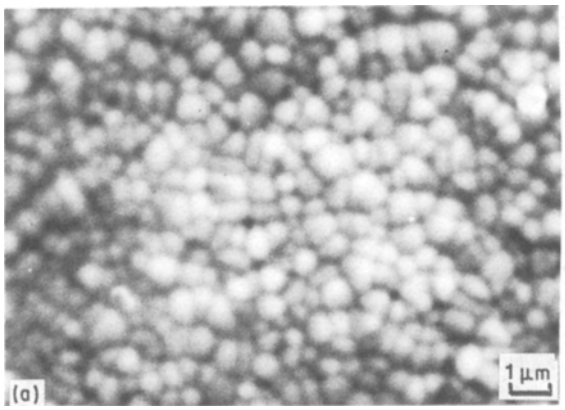

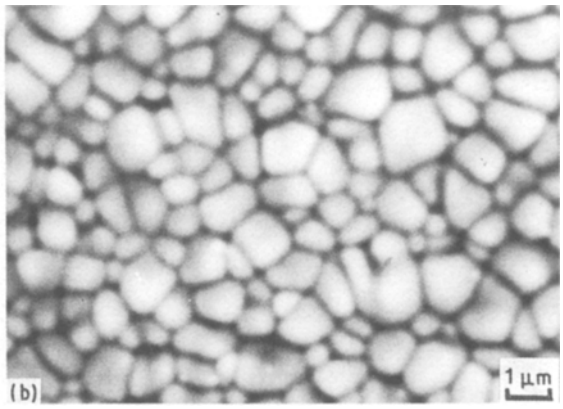

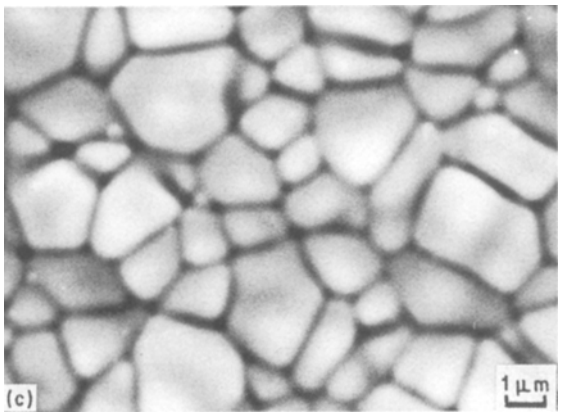

Figure 6 Plan view showing polygonal cells of as-sealed layer processed at different pulsed energy (plan view): (a) 1 J, (b) 5 J, and (c) 10 J.

appearance and topography between as-sealed and as-sprayed layers are clearly illustrated in Fig. 4 which shows the interface between a sealed region and the surrounding as-sprayed coating. The sealed zones consist of a dense completely resolidified layer (Fig. 5) and show a fine cell structure (Fig. 6). The depth of the sealed region is increased with increasing energy. However, as shown in Figs 3 and 4, there are numerous large (15 to 180 μm) diameter surface depressions. These depressions are very shallow, less than ~ 3 μm in depth. In most cases the SEM observations showed a very fine cell structure at the bottom of the depressions, but in some cases no cell structure was revealed; the depressions will be discussed more fully later. The sealed regions also contained a network of cracks but negligible porosity was observed as demonstrated by the cross-section of the sealed region in Fig. 5. The microhardness of the sealed regions was very high (~ 1450 H_v).

The pulse length has marked effects on the dimensions and microstructural features of the sealed re-

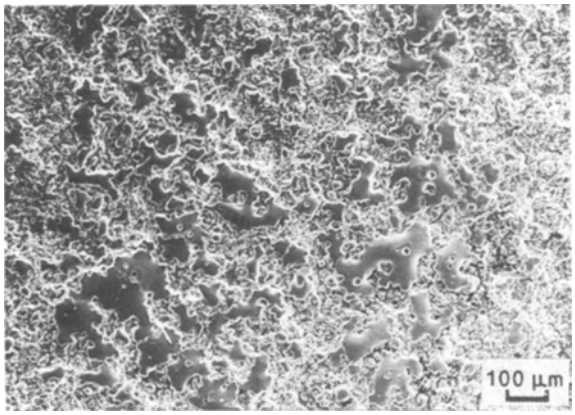

Figure 7 Plan view of partially sealed layer processed by using CW mode; specific energy, 0.79 J mm^{-2}.

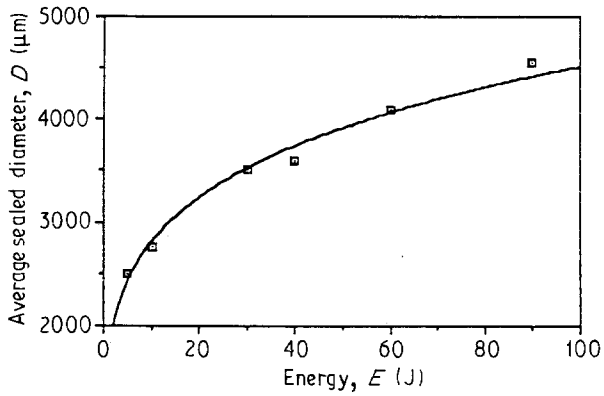

Figure 8 Variation of average sealed region diameter as a function of pulsed energy.

TABLE II Comparison of the sealing performance of pulsed and CW CO_2 laser

Interaction time (msec)	Energy (J)	Power density (W mm^{-2})	Specific energy (J mm^{-2})	Laser type	Comments
1	1	83.7	0.082	P_s	Partial sealing
10	10	51	0.4	CW	Partial sealing
21	16.8	41	0.79	CW	Partial sealing
2	2	83.7	0.167	P_s	Complete sealing
13	13	51	0.54	CW	Complete sealing
28	20.4	41	0.9	CW	Complete sealing

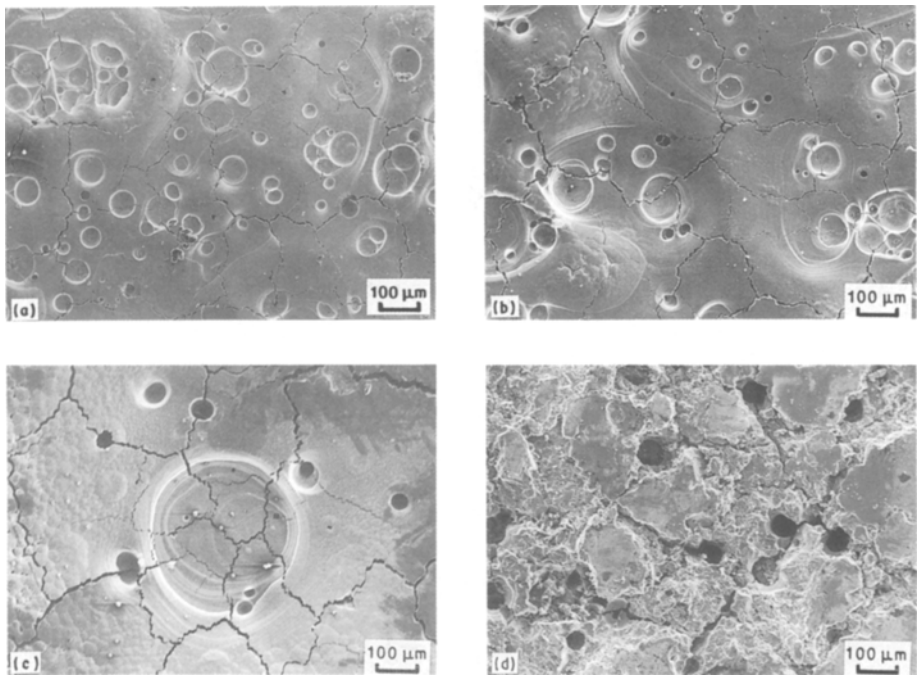

Figure 9 Plan view of sealed layers showing the crack width dependence of the pulsed energy: (a) 5 J, (b) 10 J, (c) 40 J and (d) 90 J.

gions. At the very low pulse length studied of 1 msec, which corresponds to 1 J energy or 0.082 J mm^{-2} specific energy at a constant power density of 83.7 W mm^{-2}, only partial sealing was observed, i.e. there were only small regions of local sealing due to the low interaction time being insufficient even for shallow melting over a substantial area. However, complete sealing of a thin layer was achieved at relatively short interaction times as low as 2 msec (2 J) at the same power density. Thus a specific energy of only 0.167 J mm^{-2} is sufficient for sealing using a pulsed laser. This value of specific energy is lower than the specific energy required to obtain sealing using a CW CO_2 laser [15, 17]. For example, at a power density of 41 W mm^{-2} and a specific energy of 0.79 J mm^{-2} only partial sealing is obtained with the CW laser (Fig. 7 and Table II).

From Fig. 8, it can be seen that the average diameter, D, of sealed regions is less than the beam diameter up to $\sim$ 50 J and increases with increasing pulse duration, and hence energy, E. A plot of log D against log E was linear indicating a power relationship between diameter and energy: $D = 3.25\,E^{0.2}$.

In the case of sealing with a continuous wave laser, a similar relationship between width and specific energy has previously been reported; the exponent was

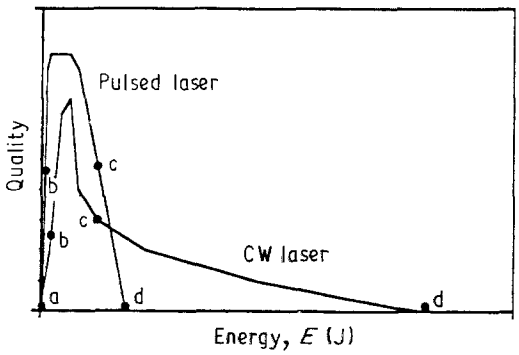

Figure 11 Schematic diagram showing the relationship between the quality of the sealed layers and energy for pulsed and continuous CO_2 lasers: (a to b) partial sealing, (b to c) acceptable sealing and (c to d) damage.

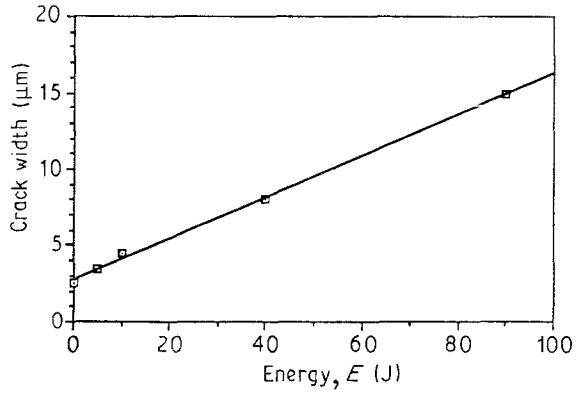

Figure 10 Relationship between crack width and energy.

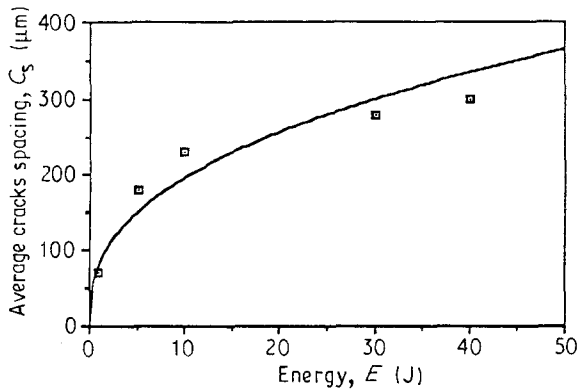

Figure 12 Relationship between the crack spacing, C_s, and energy, E.

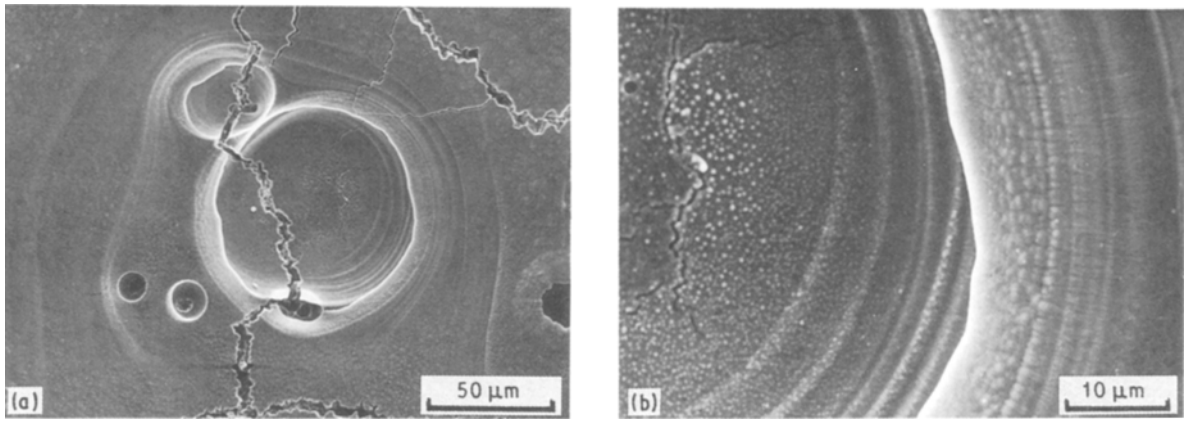

Figure 13 Scanning electron micrographs of plan view showing rippling effects and fine cell size: (a) low magnification and (b) higher magnification.

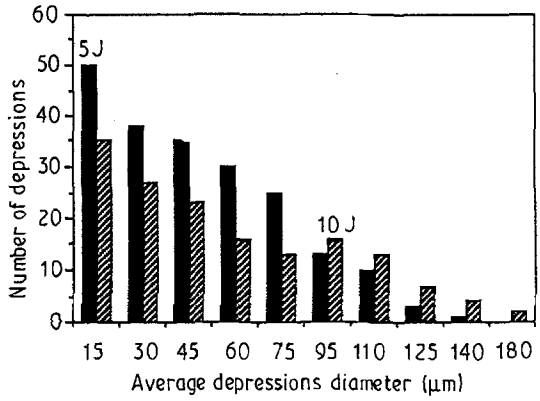

Figure 14 Statistical distribution of the number of depressions and size as a function of pulsed energy.

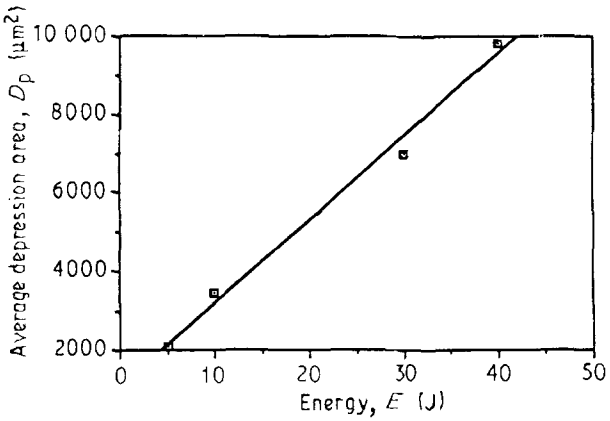

Figure 15 Relationship between the average depression area and energy.

0.3 and 0.2 for CaO-stabilized and Y_2O_3-stabilized zirconia, respectively [11, 15].

At energies greater than the minimum required for complete sealing (2 J), complete sealing was still observed but the crack width, defined as the distance between the faces of a crack, was increased (Fig. 9). Fig. 10 shows the relationship between crack width and energy; the crack width remains below approximately 8 μm for the optimum energy (5 to 40 J) but reaches nearly 15 μm for the largest pulsed energy used of 90 J. An interesting observation is that the width of the cracks is always less in the pulsed mode as compared with CW laser treatment for similar conditions. Moreover, in pulsed mode the crack density and damage of the layer is less sensitive to interaction times than in the CW mode. In the range of energy below the point of intersection of the two curves in Fig. 11, using a CW mode, the sealed layer was of a lower quality and showed a greater variability of quality (Fig. 11). Also higher energies are required in CW treatments to achieve a quality comparable with pulse treatments beyond the intersection of the two curves in Fig. 11 . This suggested that the temperature rise for a given interaction time (or given energy or specific energy) is greater for the pulsed mode.

It was also observed that the pulse energy has a dramatic effect on the spacing between cracks, C_s, which is defined as the average size of the crack network spacing (Fig. 9). At pulse energies of less than 50 J, the crack spacing, C_s, increases with energy (Fig. 12); however, at higher pulsed energy (e.g. 90 J) C_s values are not available as the network of cracks was ill-defined because of severe damage to the layer (Fig. 9d). The relationship between the C_s and pulse energy at energies below 50 J is satisfactorily described by a power law $C_s = 1.9\,E^{0.38}$.

All the depressions show rippling effects around their perimeters (Fig. 13). A small fraction of depressions with no discernible cell structure at the inner surface was seen at low energy (2 to 40 J). On increasing the energy the ratio of these depressions to depressions associated with a fine cell structure increased; however, the ratio remained much less than in the case of CW laser treatment. It should be noted that the fine cell structure present in most of the depressions was much smaller than that in the surrounding sealed region (Fig. 13). In the optimum sealing range (2 to 40 J), the number of depressions per total area of sealing decreased with increasing energy (Fig. 14). However, the proportion of total area of depressions to total area of sealing per pulse is nearly independent of energy at ~ 9% to 11% because the average size of the depressions increases with energy. The relationship between the average depression size, expressed in terms of area, D_p, as a function of energy, E, is shown in Fig. 15. The data of Fig. 15 can be described by $D_p = 2.81\,E^{0.72}$.

The mechanism of formation of depressions is not well understood, but it is suggested that it may be

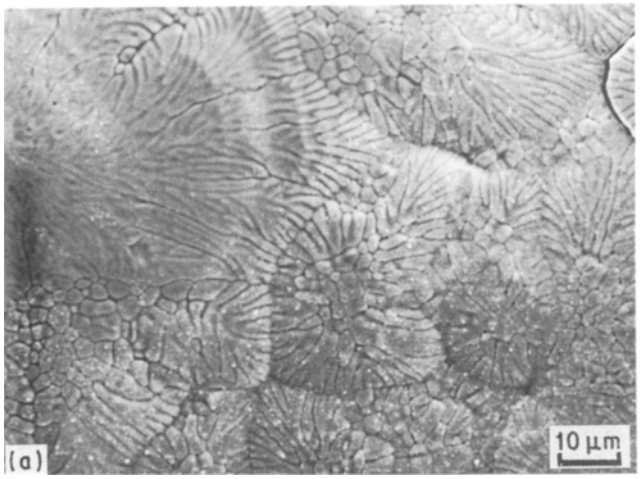

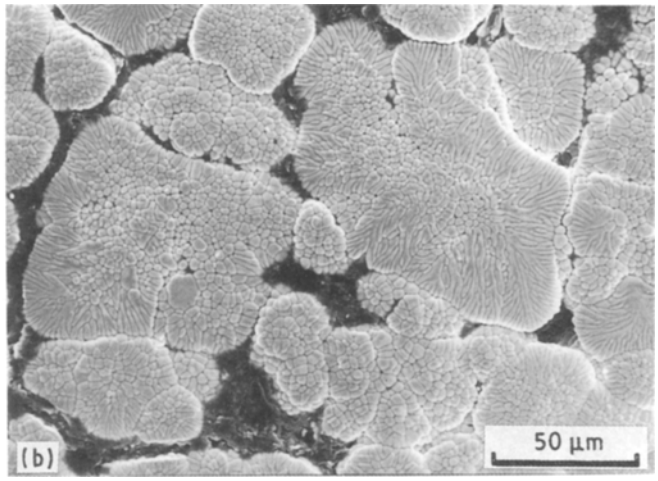

Figure 16 Some types of microstructure observed in some regions of sealed layer.

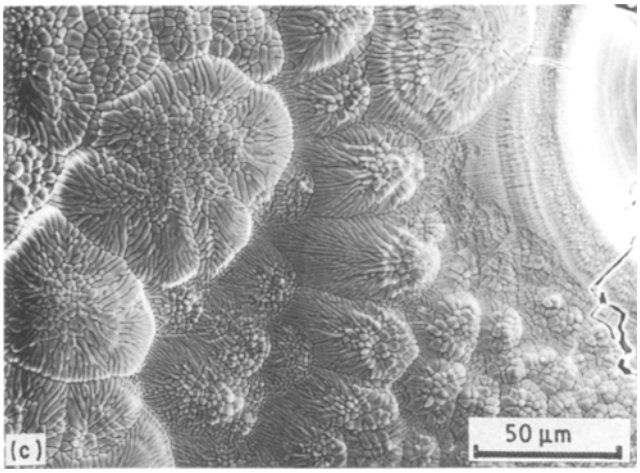

bubbles, which escape upwards through the molten ceramic layer, is a probable mechanism. With higher energy and increased interaction time and greater depth of melting, an increase in the volume of gases produced and hence of bubble size may occur. The fact that the proportion of depression area to sealed area remains approximately constant may be interpreted as due to the escape of a greater proportion of the evolved gas, consequent on easier "flotation" of large bubbles upward through the sealed zone. Consistent with the proposed mechanism was that samples pre-related to the release of expanding hot gases from the plasma-sprayed layer. The association of gases into heated prior to laser processing had a much reduced depression density that approached zero. The pre-heating drives absorbed species and gases out of the plasma coating, thus reducing the availability of gas for bubble formation during laser processing [16]. The fine cell size in the depressions indicates more rapid heat transfer in these regions and the rippling pattern is indicative of periodic liquid flow into the depressions as the gas escapes.

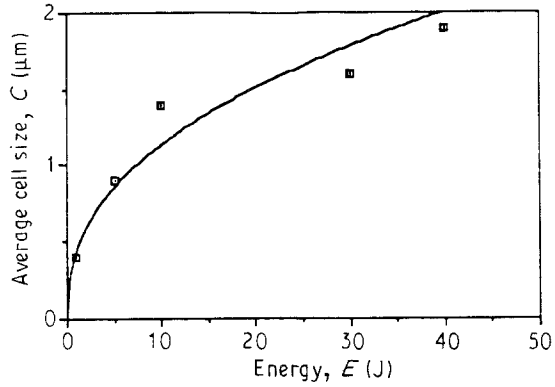

Figure 17 Relationship between cell size and energy.

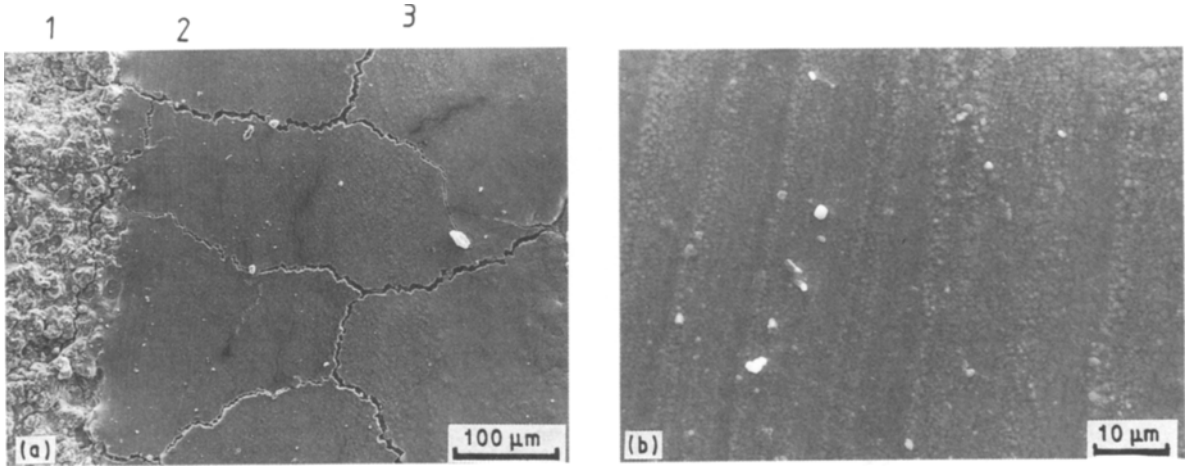

Figure 18 Scanning electron micrographs showing the rippling effect near the as-sprayed layer: (a) Low magnification: 1, as-sprayed; 2, rippling zone; and 3, sealed zone. (b) Higher magnification of the rippling zone.

In general, laser-sealed regions have a fine cell or dendritic structure which depends on the energy (cooling rate) (Fig. 16). The typical structure observed in at least 95% of the sealed region consisted of fine polyhedral cells as shown in Fig. 6. The cell size, C, increases with energy (Fig. 17); however, as previously mentioned, even at low energies the cell size is greater than that of the cells inside the depressions (Fig. 13). As for the dimensions and other microstructural features discussed in this paper, a power law adequately describes the energy, E, dependence of the cell size: $C = -0.34 E^{0.4}$.

A rippling effect was observed at high specific energy near the interface between the plasma-sprayed layer and the sealed layer due to surface tension effects between the centre and edges of the sealed zone (Fig. 18). Similar surface effects have previously been observed in laser cladding of an 8 wt % YPSZ [19].

4. Conclusion

This work has shown that pulse laser processing is capable of producing shiny surfaces of low roughness on a plasma-sprayed zirconia coating. The sealed layer has a network of cracks, but both the crack width and crack density were less than that observed with continuous wave laser processing under similar conditions. Depressions within sealed regions, which were attributed to gas evolution and bubble formation, were present but are not considered detrimental as they were shallow.

5. Acknowledgements

The authors thank Professor D. W. Pashley, Head of the Department, for providing the facilities of the laser laboratory, Mr R. Sweeney, Department of Materials, Imperial College for assistance and cooperation during this investigation, and Professor W. M. Steen, University of Liverpool, and Dr P. Chandler, Plasma Technik Ltd for the supply of plasma-sprayed samples. One of the authors (K. M. J.) thanks the Government of the Republic of Iraq, and Scientific Research Council, Baghdad and the Committee of Vice-Chancellors and Principals of the Universities of the United Kingdom for awarding a scholarship.

References

1. W. J. BRINDLEY and R. A. MILLER, *Adv. Mater. Proc.* **136** (1989) 29.
2. J. W. VOGAN, L. HSU and A. R. STETSON, *Thin Solid Films* **84** (1981) 75.
3. F. VASILIV, V. PENCEA, V. MANOLIV, I. DINCA and C. SARBU, *Amer. Ceram. Soc. Bull.* **64** (1985) 1268.
4. E. P. BUTLER, *J. Mater. Sci. Technol.* **1** (1985) 417.
5. P. CHAGNON and P. FAUCHAIS, *Ceram. Int.* **10** (1984) 119.
6. R. F. SMART and J. A. CATHERALL, "Plasma Spraying" (Mills and Boon, London, 1972) pp. 55–68.
7. D. P. H. HASSELMAN and P. S. JITENDRA, *Ceram. Bull.* **58** (1979) 856.
8. R. D. MAIER, C. M. SCHEUERMANN and C. W. ANDREWS, *ibid.* **60** (1981) 555.
9. S. R. SAUNDERS and J. R. NICHOLLS, *J. Mater. Sci. Technol.* **5** (1989) 780.
10. K. MOHAMMED JASIM, D. R. F. WEST and W. M. STEEN, *J. Mater. Sci. Lett.* **7** (1988) 1307.
11. K. MOHAMMED JASIM, D. R. F. WEST and R. D. RAWLINGS, in "Laser Processing for Industry (Laser 5)", edited by A. N. Lari and S. K. Ghosh, (iitt, France, 1989) p. 90.
12. P. A. MILLER and C. C. BERNDT, *Thin Solid Films* **119** (1984) 195.
13. I. Z. ZAPLATYNSKY, *ibid.* **95** (1982) 275.
14. R. SIVAKUMAR and B. L. MORDIKE, *Surf. Engng* **2** (1988) 127.
15. K. MOHAMMED JASIM, D. R. F. WEST, W. M. STEEN and R. D. RAWLINGS, Laser Materials Processing ("ICALEO '88") edited by G. Bruck (Springer–Verlag IFS (Publications) Ltd. UK in association with Laser Institute of America, 1989)
16. K. MOHAMMED JASIM, R. D. RAWLINGS and D. R. F. WEST, unpublished work, 1989.
17. F. S. GALSASSO and K. VEELTRI, *Ceram. Bull.* **2** (1983) 253.
18. S. DALLAIRE and P. CIELO, *Metall. Trans.* **13B** (1982) 497.
19. K. MOHAMMED JASIM, R. D. RAWLINGS and D. R. F. WEST, *J. Mater. Sci.* **25** (1990) 15.

Received 15 March
and accepted 29 March 1990